Supporting Information

Restriction of Ce-MOF growth within ZSM zeolite for robust three-proofing thermoplastic polyurethane

Xue Bi[a,d], Kunpeng Song[a], Qianlong Li[a], Tao Lin[b], Ye-Tang Pan[a]*, Wei Wang[c], Jiyu He[a]*, Rongjie Yang[a,d]

[a] *National Engineering Research Center of Flame Retardant Materials, School of Materials Science & Engineering, Beijing Institute of Technology, Beijing 100081, PR China.*

[b] *School Material Science & Engineering, Tsinghua University, Beijing 100084, Peoples R China.*

[c] *School of Computer Science and Engineering, The University of New South Wales, Sydney, New South Wales 2052, Australia.*

[d] *Zhongyuan Research Center for Flame Retardant Materials, Beijing Institute of Technology, Xuchang 461000, Henan, China.*

*Corresponding author: Ye-Tang Pan; Jiyu He.

E-mail address: pyt@bit.edu.cn; hejiyu@bit.edu.cn

Characterization

X-ray diffraction (XRD) was employed on an X-ray diffractometer (DX-2600, Rigaku, Tokyo, Japan), using Cu Kα radiation (Kλ=1.5418 Å), at a scanning rate of 0.01 °/s.

Scanning electron microscope (SEM) and Energy dispersive X-ray spectrometry were performed on a Regulus8230 (Hitachi, Japan) at the accelerating voltage of 15 kV. Electron Distribution Spectroscopy (EDS) was performed with X-Max (Oxford).

Transmission electron microscopy (TEM) was employed on a Tecnai G2 F20 S-TWIN (FEI, America) at 300 kV and a tungsten filament transmission electron microscope (JEM 1200EX, JEOL, Japan) operated at 100 kV. The carbon membrane support was supplied by Beijing Zhongjingkeyi Technology Co. Ltd.

X-Ray photoelectron spectroscopy (XPS) spectra was conducted by using an Thermo Scientific K-Alpha X-ray photoelectron spectrometer (Thermo Fisher Scientific).

The nitrogen sorption isotherms of the samples were examined using an ASAP 2460 analyzer (MICROMERITICS INSTRUMENT CORP, USA) employing the BET method.

Raman spectroscopy was studied the structure components of the residual char of PUA composites by a Renishaw in Via confocal microscope Raman system (Renishaw, UK) with a 633 nm laser source. The authors extend their gratitude to Mr. Shuai Xingpeng from Shiyanjia Lab (www.shiyanjia.com) for providing invaluable assistance with the Raman analysis.

Thermogravimetric analysis (TGA) was performed by using a thermogravimetric analyzer (Mettler-Toledo, Zurich, Switzerland) with the specimen weight of 8 mg at a heating rate of 10℃/min under nitrogen.

Limiting oxygen index (LOI) was tested by g an oxygen index analyzer (Rheometric Scientific Ltd., Hampshire, UK) with the specimen dimension of 130 × 6.5 × 3 mm^3 according to ASTM D 2863 procedure.

Cone calorimeter test (cone) was performed to study the fire performance of PUA

composites according to the standard of ISO 5660 by a microscale combustion calorimeter (GOVMARKMCC-2) at a heat flux of 50 kW/m^2.

Thermogravimetric analysis-infrared spectrometry (TG-IR) was performed using a STA 8000 thermogravimetric analyzer (Perkin Elmer) interfaced to the Frontier FT-IR spectrophotometer (Perkin Elmer) at a heating rate of 10°C/min under nitrogen. The FT-IR specimen cell was kept at 280°C.

The hardness of all TPU materials was assessed using a Shore hardness tester (HPE II, Bareiss) and averaged over the five points of each sample.

The contact angle of all fillers and TPU materials with water, as well as the contact angle of all fillers with ethylene glycol, was evaluated using a contact angle meter (Germany-Dataphysics-OCA20) and averaged the two points for each sample.

The UV-vis absorption spectra of TPU samples were measured using a UH4100 spectrometer (Hitachi, Japan) in the range of 200-900 nm at room temperature.

The mechanical properties of the splines were tested using an electronic tensile testing machine (DXLL-5000, Shanghai D & G Measure Instrument Co. Ltd., China) operated at a rate of 10 mm/min.

Differential scanning calorimetry (DSC) measurements were performed with DSC214 (NETZSCH, Germany) at a heating rate of 10°C/min and a cooling rate of 5°C/min. The specific test process is to raise the temperature to 250°C, then cool down to -100°C, and then increase the temperature to 250°C.

Results and discussions

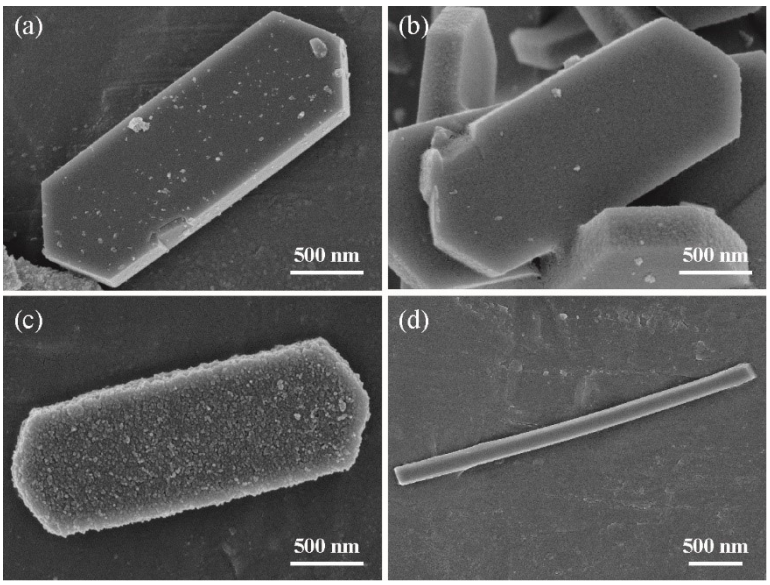

Figure S1. SEM image of (a) ZSM-5, (b) Ce@ZSM-5, (c) Ce-MOF@ZSM-5 and (d) Ce-MOF.

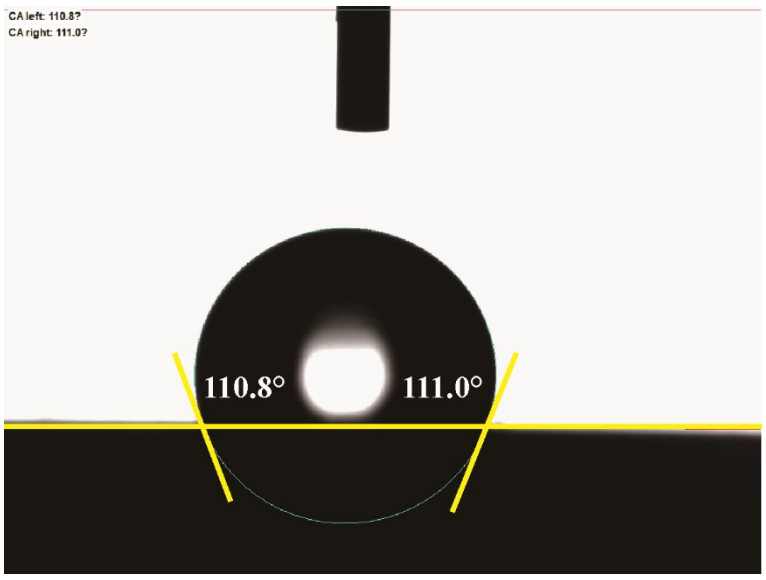

Figure S2. Water contact angles of pure TPU.

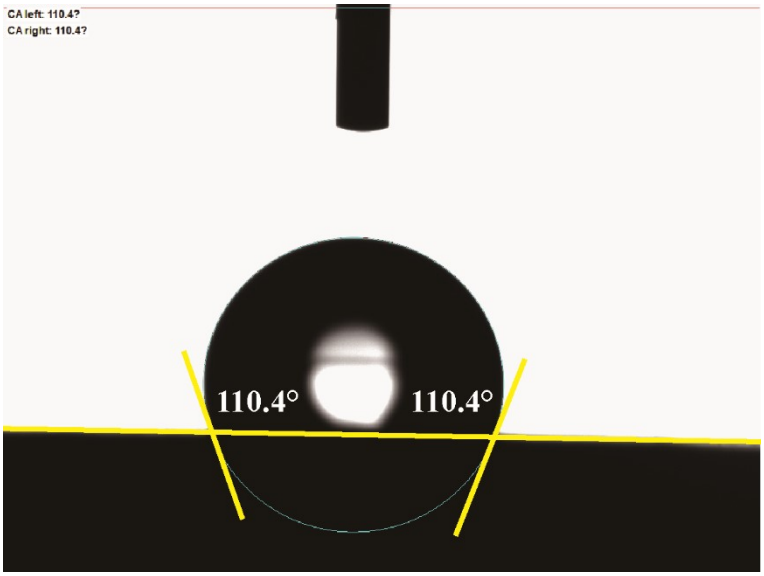

Figure S3. Water contact angles of TPU/ZSM-5.

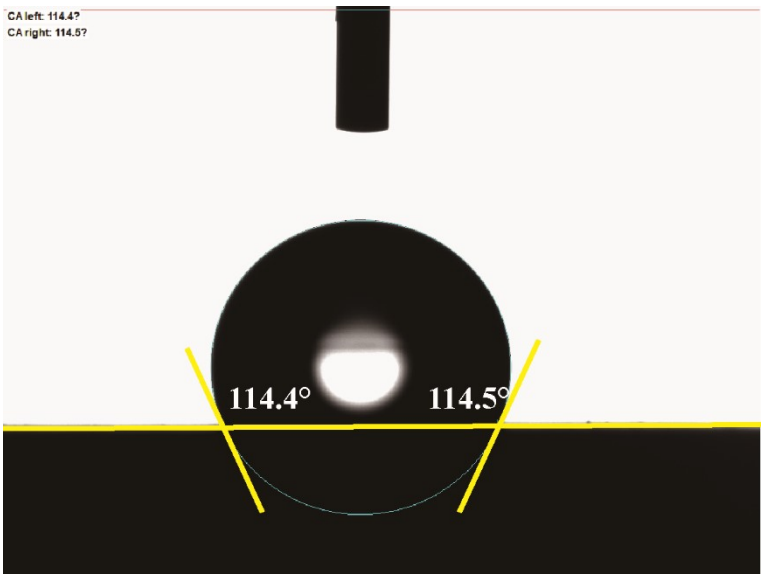

Figure S4. Water contact angles of TPU/Ce@ZSM-5.

Figure S5. Water contact angles of TPU/Ce-MOF.

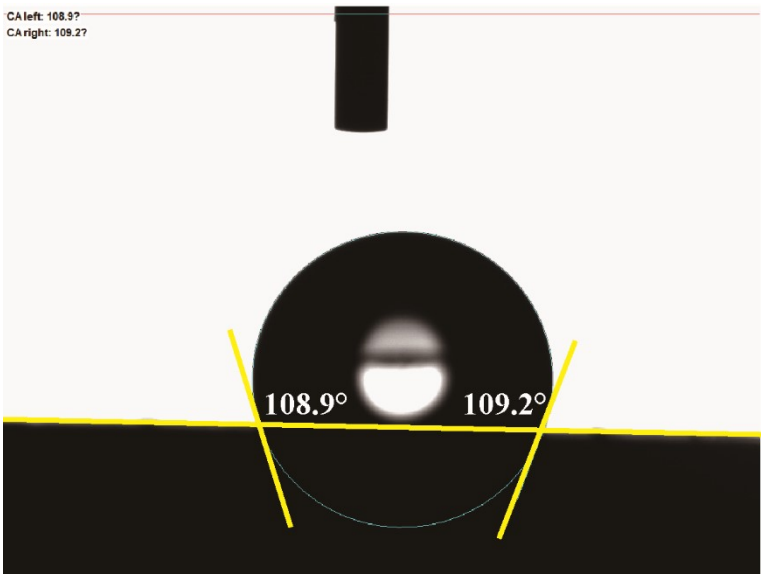

Figure S6. Water contact angles of TPU/Ce-MOF@ZSM-5.

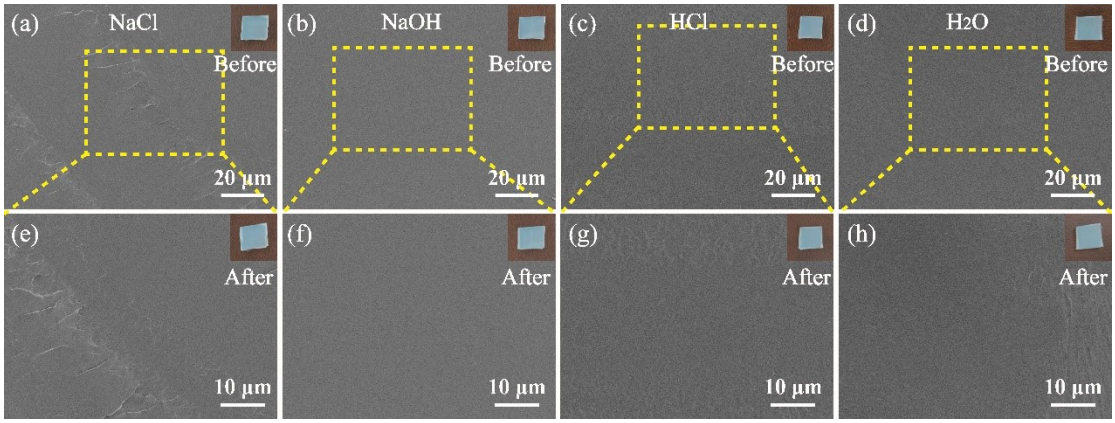

Figure S7. SEM image and enlarged SEM image of the fractured surface of pure TPU after 60 days of the chemical resistance test.

Table S1. Thermal decomposition data of hybrid materials in N_2.

Samples	$T_{5\%}$ (°C)	T_{max} (°C)	R_{max} (%/°C)	$Char_{800°C}$ (%)
ZSM-5	-	-	-	95.6
Ce@ZSM-5	284.3	-	-	92.9
Ce-MOF	99.6	-4.16	108.1	55.6
Ce-MOF@ZSM-5	603.8	-	-	94.5

Table S2. Contact angle data of TPU and TPU composites.

Sample	Contact angle (degrees)
pure TPU	110.9±2.6
TPU/ZSM-5	110.4±1.7
TPU/Ce@ZSM-5	114.4±2.1
TPU/Ce-MOF	110.8±1.5
TPU/Ce-MOF@ZSM-5	109.0±1.2

Table S3. Contact angle data and surface energy results for TPU and the hybrids.

Sample	Contact angle (degrees)		γ_{SV}^{d}	γ_{SV}^{p}	γ_{SV}	γ_{12}
	θ（water）	θ（ethylene glycol）	($MJ \cdot m^{-2}$)	($MJ \cdot m^{-2}$)	($MJ \cdot m^{-2}$)	($MJ \cdot m^{-2}$)
pure TPU	110.9±2.6	89.7±1.5	15.21	0.53	15.74	-
ZSM-5	18.6±0.3	26.7±0.2	0.90	86.64	87.54	82.33
Ce@ZSM-5	20.7±0.5	36.5±0.4	0.04	94.65	94.69	80.54
Ce-MOF	32.4±0.6	33.5±0.2	1.66	73.26	74.92	68.15
Ce-MOF@ZSM-5	29.9±1.1	31.9±0.3	3.91	67.64	71.55	59.89

Table S4. Tensile strength and Elongation of TPU and TPU composites.

Sample	Tensile strength (MPa)	Elongation at the break (%)
pure TPU	28.58±1.08	432.05±15.26
TPU/ZSM-5	24.52±1.06	338.86±10.24
TPU/Ce@ZSM-5	22.68±0.95	335.29±11.08
TPU/Ce-MOF	18.95±1.05	301.06±10.49
TPU/Ce-MOF@ZSM-5	27.18±1.34	412.50±16.32

Table S5. Comparison of tensile strength and elongation at break TPU/Ce-

MOF@ZSM-5 nanocomposites with other TPU nanocomposites previously reported.

Samples	Contents	Tensile strength ($kW \cdot m^{-2}$)	Elongation at break ($MJ \cdot m^{-2}$)	Ref.
TPU/f-Ti_3C_2-3.0	3 wt.%	+31.2%	-30.3%	[1]
TPU/f-BN-5.0	5 wt.%	+39.4%	-44.3%	[2]
TPU/3.0 CPBN	3 wt.%	+38.1%	-6.2%	[3]
TPU/AHP/PMT	10%	/	-24.3%	[4]
TPU/15 wt.% DMPY	15 wt.%	-29.5%	-31.9%	[5]
PU/6.5APP/0.5ZIF-67@GO	7%	-25.9%	-27.7%	[6]
TPU/6AHP/1NiFe-LDH	7%	-6.0%	-6.9%	[7]
TPU/MXene@SiC@PANI	5 wt.%	-4.9%	-4.5%	This work

Table S6. Shore hardness data of TPU and TPU composites.

Sample	1	2	3	4	5	Average value
pure TPU	90.6	90.1	90.4	90.8	90.3	90.4
TPU/ZSM-5	92.7	92.5	92.5	92.8	92.4	92.6
TPU/Ce@ZSM-5	92.1	92.3	92.4	91.8	92.5	92.2
TPU/Ce-MOF	91.7	91.8	92.3	92.1	91.7	91.9
TPU/Ce-MOF@ZSM-5	92.6	92.2	91.9	92.4	92.1	92.2

Table S7. Thermal decomposition data of TPU and TPU composites after 12 h UV

irradiation.

Samples	$T_{5\%}$ (°C)	T_{max} (°C)	R_{max} (%/°C)	$Char_{800°C}$ (%)
pure TPU	290.5	401.8	-1.07	7.1
TPU/ZSM-5	294.8	406.7	-1.17	13.2
TPU/Ce@ZSM-5	293.3	408.7	-1.02	11.2
TPU/Ce-MOF	295.0	402.2	-1.27	10.6
TPU/Ce-MOF@ZSM-5	291.8	411.3	-1.00	15.1

Table S8. Tensile strength and Elongation of TPU and TPU composites after 12 h UV irradiation.

Sample	Tensile strength (MPa)	Elongation at the break (%)	Retention of tensile strength (%)	Retention of elongation at break (%)
pure TPU	8.03±0.59	109.09±10.34	28.10	25.25
TPU/ZSM-5	22.81±1.16	328.49±15.27	93.03	96.94
TPU/Ce@ZSM-5	19.71±0.86	291.85±11.05	86.90	87.04
TPU/Ce-MOF	12.06±0.49	132.80±5.48	63.64	44.11
TPU/Ce-MOF@ZSM-5	26.88±1.35	401.21±16.29	98.89	97.74

Table S9. Weight changes curves of pure TPU in 3.5 wt.% NaCl aqueous solution, 3.5 wt.% NaOH aqueous solution, 3.5 wt.% HCl solution and deionized water.

Times (day)	NaCl (wt. %)	NaOH (wt. %)	HCl (wt. %)	H_2O (wt. %)
10	1.318	1.353	1.311	1.266
20	2.031	2.297	2.265	1.931
30	2.405	2.861	2.772	2.293
40	2.637	3.133	3.032	2.566
50	2.812	3.253	3.231	2.698
60	2.926	3.371	3.313	2.808

Table S10. Weight changes curves of TPU/Ce-MOF@ZSM-5 in 3.5 wt.% NaCl aqueous solution, 3.5 wt.% NaOH aqueous solution, 3.5 wt.% HCl solution and deionized water.

Times (day)	NaCl (wt. %)	NaOH (wt. %)	HCl (wt. %)	H_2O (wt. %)
10	0.787	0.792	0.821	0.572
20	1.126	1.292	1.329	0.953
30	1.448	1.721	1.652	1.410
40	1.764	1.984	1.973	1.702
50	1.895	2.229	2.232	1.922
60	2.003	2.310	2.391	2.030

Table S11. Thermal decomposition data of TPU and TPU composites.

Samples	$T_{5\%}$ (°C)	T_{max} (°C)	R_{max} (%/°C)	$Char_{800°C}$ (%)
pure TPU	290.5	407.8	-1.00	8.2
TPU/ZSM-5	293.3	417.3	-0.96	13.8
TPU/Ce@ZSM-5	294.8	416.3	-1.01	12.4
TPU/Ce-MOF	295.0	407.8	-1.01	11.2
TPU/Ce-MOF@ZSM-5	291.8	409.3	-0.98	15.3

Table S12. Combustion parameters after cone of TPU and TPU composites.

Samples	pure TPU	TPU/ZSM-5	TPU/Ce@ZSM-5	TPU/Ce-MOF	TPU/ Ce-MOF@ZSM-5
LOI (%)	21.2	23.2	23.0	23.5	24.3
pHRR (kW/m^2)	1124±31	931±19	1019±27	1071±25	832±16
THR (MJ/m^2)	87±9	78±7	78±6	83±7	69±5
pSPR (m^2/kg)	0.164±0.011	0.121±0.008	0.122±0.009	0.111±0.007	0.107±0.008
TSP (m^2)	14.66±0.6	12.98±0.7	11.35±0.4	12.41±0.5	10.93±0.5
tpSPR (s)	105±7	125±5	100±5	100±4	95±6
pCOP (g/s)	0.0129±0.0010	0.0089±0.0009	0.0094±0.0007	0.0095±0.0004	0.0078±0.0005
pCO_2P (g/s)	0.74±0.12	0.54±0.08	0.62±0.05	0.64±0.10	0.53±0.06
Residue (%)	3.5±0.5	10.4±1.2	16.3±1.2	9.2±0.7	25.1±1.9

Table S13. Comparison of heat release, smoke release of TPU/Ce-MOF@ZSM-5

nanocomposites with other TPU nanocomposites previously reported.

Samples	Contents	pHRR (kW/m^2)	THR (MJ/m^2)	pSPR (m^2/kg)	TSP (m^2)	Ref.
Co@PCN-TPU	3 wt.%	-16.4%	-11.2%	-21.8%	/	[8]
CNPPy-TPU	3%	-29.8%	-28.3%	-28.7%	-24.2%	[9]
TPU/BNNO@Co_3O_4@PPZ	2 wt.%	-44.1%	-10.4%	-51.2%	-20.4%	[10]
TPU/MXene@SnO_2-2	2 wt.%	-50.5%	-9.7%	-35.1%	-16.3%	[11]
SW-Si_3N_4/TPU	3%	-27.4%	-28.2%	/	/	[12]
Co_3O_4-GNS	2 wt.%	-16.4%	/	/	/	[13]
TPU/Ce-MOF@ZSM-5	5 wt.%	-26.0%	-20.7%	-34.8%	-25.4%	This work

Table S14. Thermal decomposition data of TPU composites.

Samples	C-C/C-H area (%)	C-O area (%)	C=O area (%)	Cox/Ca
Pure TPU	55.58	25.54	18.89	79.94
TPU/Ce-MOF@ZSM-5	57.85	25.93	16.23	72.88

1. L. He, J. Wang, B. Wang, X. Wang, X. Zhou, W. Cai, X. Mu, Y. Hou, Y. Hu and L. Song, *Compos. B. Eng.*, 2019, **179**, 107486.

2. W. Cai, N. Hong, X. Feng, W. Zeng, Y. Shi, Y. Zhang, B. Wang and Y. Hu, *Chem. Eng. J.*, 2017, **330**, 309-321.
3. J. Wang, D. Zhang, Y. Zhang, W. Cai, C. Yao, Y. Hu and W. Hu, *J. Hazard. Mater.*, 2019, **362**, 482-494.
4. X. Liu, J. Guo, W. Tang, H. Li, X. Gu, J. Sun and S. Zhang, *Compos. Part A Appl. Sci. Manuf.*, 2019, **119**, 291-298.
5. L. Liu, Y. Xu, Y. He, M. Xu, Z. Shi, H. Hu, Z. Yang and B. Li, *Polym. Degrad. Stab.*, 2019, **167**, 146-156.
6. Q. Liu, H. Wang, H. Li, J. Sun, X. Gu and S. Zhang, *Polym. Adv. Technol.*, 2022, **33**, 2374-2385.
7. S. Xu, J. Liu, X. Liu, H. Li, X. Gu, J. Sun and S. Zhang, *Polym. Degrad. Stab.*, 2022, **202**, 110043.
8. E. Szliszka, Z. P. Czuba, M. Domino, B. Mazur, G. Zydowicz and W. Krol, *Molecules*, 2009, **14**, 738-754.
9. S. Lu, H. Shi, B. Shen, W. Hong, D. Yu and X. Chen, *J. Polym. Res.*, 2022, **29**, 263.
10. Y. Tong, W. Wu, W. Zhao, Y. Xing, H. Zhang, C. Wang, T. B. Y. Chen, A. C. Y. Yuen, B. Yu, X. Cao and X. Yi, *Polymers*, 2022, **14**, 4341.
11. W. Cai, Z. Li, T. Cui, X. Feng, L. Song, Y. Hu and X. Wang, *Composites Part B: Engineering*, 2022, **244**, 110204.
12. L. Cheng, J. Wang, S. Qiu, J. Wang, Y. Zhou, L. Han, B. Zou, Z. Xu, Y. Hu and C. Ma, *J. Colloid Interface Sci.*, 2021, **603**, 844-855.
13. K. Zhou, Z. Gui, Y. Hu, S. Jiang and G. Tang, *Compos. Part A Appl. Sci. Manuf.*, 2016, **88**, 10-18.